AGU PUBLICATIONS

Geophysical Research Letters

RESEARCH LETTER

10.1002/2015GL064057

Key Points:
- Oscillatory flow braking in the Earth's magnetotail may be anharmonic
- This explains the first harmonic observations in Pi2 pulsations on the ground
- Harmonic generation enriches the nature of the M-I coupling

Correspondence to:
E. V. Panov,
evgeny.panov@oeaw.ac.at

Citation:
Panov, E. V., R. A. Wolf, M. V. Kubyshkina, R. Nakamura, and W. Baumjohann (2015), Anharmonic oscillatory flow braking in the Earth's magnetotail, *Geophys. Res. Lett.*, *42*, 3700–3706, doi:10.1002/2015GL064057.

Received 31 MAR 2015
Accepted 17 APR 2015
Accepted article online 22 APR 2015
Published online 25 MAY 2015
Corrected 29 JUN 2015

This article was corrected on 29 JUN 2015. See the end of the full text for details.

Anharmonic oscillatory flow braking in the Earth's magnetotail

E. V. Panov[1], R. A. Wolf[2], M. V. Kubyshkina[3], R. Nakamura[1], and W. Baumjohann[1]

[1]Space Research Institute, Austrian Academy of Sciences, Graz, Austria, [2]Physics and Astronomy Department, William Marsh Rice University, Houston, Texas, USA, [3]Institute of Physics, St. Petersburg State University, St. Petersburg, Russia

Abstract Plasma sheet bursty bulk flows often oscillate around their equilibrium position at about 10 R_E downtail. The radial magnetic field, pressure, and flux tube volume profiles usually behave differently earthward and tailward of this position. Using data from five Time History of Events and Macroscale Interactions during Substorms (THEMIS) probes, we reconstruct these profiles with the help of an empirical model and apply thin filament theory to show that the oscillatory flow braking can occur in an asymmetric potential. Thus, the thin filament oscillations appear to be anharmonic, with a power spectrum exhibiting peaks at both the fundamental frequency and the first harmonic. Such anharmonic oscillatory braking can explain the presence of the first harmonic in Pi2 pulsations (frequency doubling), which are simultaneously observed by magnetometers on the ground near the conjugate THEMIS footprints.

1. Introduction

Bursty bulk flows (BBFs) [*Baumjohann et al.*, 1990; *Angelopoulos et al.*, 1994] are believed to provide magnetic flux transport to overcome the pressure balance inconsistency [*Erickson and Wolf*, 1980; *Pontius and Wolf*, 1990; *Yang et al.*, 2014] and may lead to a substorm current wedge [*Baumjohann et al.*, 1991; *Shiokawa et al.*, 1997; *Birn et al.*, 1999; *Ohtani et al.*, 2009; *Nishimura et al.*, 2010] and substorm onset. The arrival of BBFs in the innermost part of the plasma sheet causes more field lines in that region to be dipolar in shape [*Nakamura et al.*, 1994; *Schödel et al.*, 2001; *Baumjohann*, 2002; *Nakamura et al.*, 2002; *Kaufmann et al.*, 2005]. Dipolarization is first observed in the near-Earth plasma sheet and then extends tailward [*Baumjohann et al.*, 1999; *Birn et al.*, 2011].

Braking of BBFs, decelerated by the dominant dipolar magnetic field at around 10 R_E downtail, can often be oscillatory [*Chen and Wolf*, 1999; *Panov et al.*, 2013]. Estimates of bursty bulk flow oscillation periods can be derived analytically in the MHD approximation using typical background plasma sheet parameters [*Wolf et al.*, 2012]. Farther out in the tail where field lines are longer, the oscillation period increases [*Wolf et al.*, 2012; *Panov et al.*, 2014a].

BBFs may lead to onset of Pi2 pulsations [*Shiokawa et al.*, 1998; *Kepko et al.*, 2001]. Periods and damping factors of Pi2 pulsations correlate with the ones of oscillatory flow braking in the magnetotail, although the presence of the first harmonic in the power spectrum of Pi2 pulsations (frequency doubling) remains puzzling [*Panov et al.*, 2014b].

Asymmetry in the radial background plasma sheet profiles of magnetic field, pressure, and flux tube volume leads to an asymmetric potential around the equilibrium position that causes anharmonicity [*Wolf et al.*, 2012]. In the case of a strong asymmetry, harmonic generation is expected to occur.

We employ Time History of Events and Macroscale Interactions during Substorms (THEMIS) [*Angelopoulos*, 2008] space (probes P1–P5) and ground magnetometer observations on 23 March 2009 between 06:00 and 06:40 UT to reveal the level of the potential asymmetry and identify the anharmonicity signatures of Pi2 pulsations during oscillatory flow braking.

Magnetotail observations were provided by the probes' fluxgate magnetometers (FGM) [*Auster et al.*, 2008] and electrostatic analyzers' [*McFadden et al.*, 2008] particle detectors. The AM03 model [*Kubyshkina et al.*, 2011] is used to reconstruct the radial magnetic field, pressure, and flux tube volume profiles in the background plasma sheet. The ground-based observations of the ionospheric magnetic field were provided by the THEMIS and Canadian Array for Realtime Investigations of Magnetic Activity (CARISMA) magnetometer arrays over North America (see *Mende et al.* [2008] and *Mann et al.* [2008] for details).

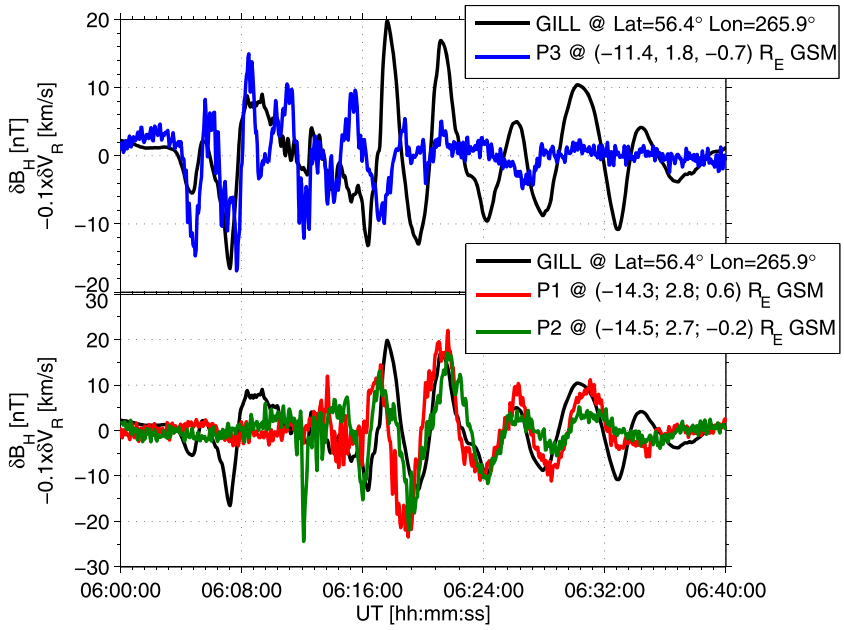

Figure 1. Oscillations in the radial velocity V_R, at P1–P3, and in the B_H component of the magnetic field at Gillam, Canada.

2. THEMIS Observations and Theoretical Expectations

Figure 1 shows the oscillations in the radial velocity V_R at P3 located about 11 R_E downtail (top) and P1 and P2 located about 14 R_E downtail (bottom) on 23 March 2009 between 6:00 and 6:40 UT. It was shown recently that these oscillations in V_R can be interpreted as signatures of a thin filament oscillation [*Panov et al.*, 2014a]. At 6:08 UT, the equilibrium position of the thin filament was near the location of P3, i.e., near $X = -11\ R_E$, whereas at 6:21 UT, the equilibrium position moved closer to the location of P1 and P2, i.e., near $X = -14\ R_E$.

The oscillatory braking of fast flows in the near-Earth plasma sheet is transmitted down to Earth and observed as Pi2 pulsations [*Panov et al.*, 2014b]. With the help of the AM03 model, we identified the location of THEMIS probes' footprints to be between Rankin Inlet and Gillam/Fort Churchill, Canada [*Panov et al.*, 2014a]. We found good agreement between P3 and Gillam (see black lines in Figure 1) between about 06:04 and 06:08 UT and between P1 and P2 and Gillam between about 06:16 and 06:32 UT. Agreement is not clear at other times. This fact is in agreement with the conclusion that between 6:08 and 6:16 UT, due to tailward expansion of flux pileup region, the oscillatory flow braking retreated tailward from $X = -11.5\ R_E$ (location of P3, cf. in Figure 1 (top)) to $X = -14\ R_E$ (location of P1 and P2, cf. in Figure 1 (bottom)) [*Panov et al.*, 2014b].

With the help of the AM03 model, we also reconstructed the radial profiles of B_Z magnetic field component, pressure, and flux tube volume in the background plasma sheet. Figure 2 shows radial profiles of the background plasma sheet parameters on 23 March 2009 predicted by the AM03 model at 6:21 UT: (a) $B_{z,e}$ magnetic field component at the neutral sheet, (b) total pressure P, (c) flux tube volume V. The AM03 model revealed that all three radial profiles of $B_{z,e}$, P, and V are not radially symmetric around $X = -14\ R_E$.

With the help of $B_{z,e}$, P, and V using equation (26) of *Wolf et al.* [2012], we applied two algorithms to analytically derive force per unit magnetic flux F_x (Figure 2d) and potential U (Figure 2e) around the equilibrium position at $X = -14\ R_E$ at 6:21 UT. Appendix A provides further details of the algorithms (specifically, cf. equations (A7) and (A9) in Appendix A). It appears that the asymmetries in $B_{z,e}$, P, and V radial profiles are the reason that the associated potential U is not symmetric about the equilibrium position. Note that formula (26) in *Wolf et al.* [2012] was derived for the tail-like configuration of the plasma sheet. The tail-like plasma sheet configuration reveals a general agreement in Figure 2 with the qualitative sketch given in Figure 8 of *Wolf et al.* [2012].

Using the obtained F_x and U, we plot the thin filament oscillation parameters around the equilibrium position at $X = -14\ R_E$ at 6:21 UT in Figure 3: (a) coordinate x, (b) velocity v, (c) phase portrait (x,v), and (d) wavelet spectrum of v. Due to asymmetry in U, the oscillation appears to be anharmonic: the oscillations of the x and v

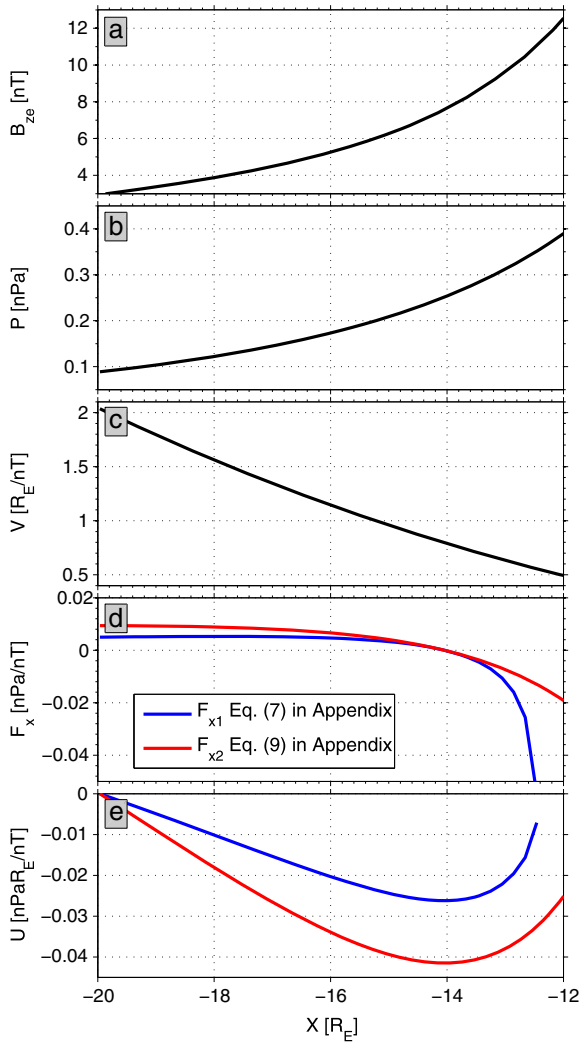

Figure 2. Radial profiles of the background plasma sheet parameters on 23 March 2009 predicted by the AM03 model at 6:21 UT: (a) vertical magnetic field component $B_{z,e}$ at the neutral sheet, (b) total pressure P, (c) flux tube volume V, (d) force per unit magnetic flux F_x, and (e) associated potential U. F_x and U were estimated for the equilibrium position at $X = -14\ R_E$ from equation (26) of *Wolf et al.* [2012] with the help of $B_{z,e}$, T, and V using two algorithms. See Appendix A for algorithm descriptions. Blue curves were calculated from equation (A7), red curves from (A9).

curves (Figures 3a and 3b) are not sinusoidal. The troughs of x are broader than the peaks, because the restoring force F_x tends to be weaker on the low-x side of equilibrium than on the high-x side. The phase portrait of the oscillation represents an egg-like shape rather than an ellipse (Figure 3c). The wavelet spectrum of v (Figure 3d) reveals two maxima with 6.2 min (fundamental mode) and 3.1 min (first harmonic) periods.

Figure 4 shows B_H magnetic field components from two other magnetometers (at Fort Churchill and Rankin Inlet in Canada) located in the vicinity of THEMIS probes footprints on 23 March 2009 between 6:00 and 6:40 UT. There B_H exhibited similar oscillations as those in B_H from Gillam, shown in Figure 1. The corresponding wavelet spectra in Figure 4 show that indeed two spectral maxima can be seen (indicated by black arrows in Figure 4). Around 6:08 UT, the oscillation period of the plasma sheet flows near the equilibrium position at about $X = -11\ R_E$ was about 3.5 min (compare with the oscillation period of the fundamental ground Pi2 oscillations in Figure 4c). Later, around 6:21 UT, the oscillation period of the plasma sheet flows near the equilibrium position that retreated tailward to about $X = -14\ R_E$ increased to about 6.2 min (compare with the oscillation period of the fundamental ground Pi2 oscillations in Figure 4d) (see *Panov et al.* [2014a] for details). The second maxima in Figures 4c and 4d correspond to the first harmonics with periods 1.8 min around 6:08 UT and 3.2 min around 6:21 UT.

3. Discussion

The velocity data from THEMIS probes in the plasma sheet represent a local plasma velocity at essentially fixed point that is observed as a function of time rather than the time-dependent velocity of a moving thin filament. Also, spacecraft velocity data in the plasma sheet generally are subject to high noise levels. These facts make it difficult to use plasma sheet velocity measurements to test whether the oscillations are harmonic. However, the statistically established fact that the signal from the oscillatory braking of fast flows in the near-Earth plasma sheet is transmitted down to Earth and is observed as Pi2 pulsations there [*Panov et al.*, 2014b] allowed us to use ground magnetometer measurements near THEMIS footprints instead, thereby suggesting anharmonicity of the flow oscillations observed by THEMIS probes P1–P3 at 11–14 R_E downtail.

Note that the signal transmission process may be rather complex and involve a mix of, e.g., magnetospheric, ionospheric, and plasmaspheric eigenmodes. For instance, *Lysak et al.* [2015] have investigated propagation of a damped sine wave with about 1 min period from the near-Earth plasma sheet ($X \approx -10\ R_E$) down to the low-altitude ionospheric boundary placed at 100 km. They have revealed that ULF waves can propagate through the inner magnetosphere, and a compressional pulse at $-10\ R_E$ can excite both shear-mode field line resonances and fast-mode plasmaspheric resonances.

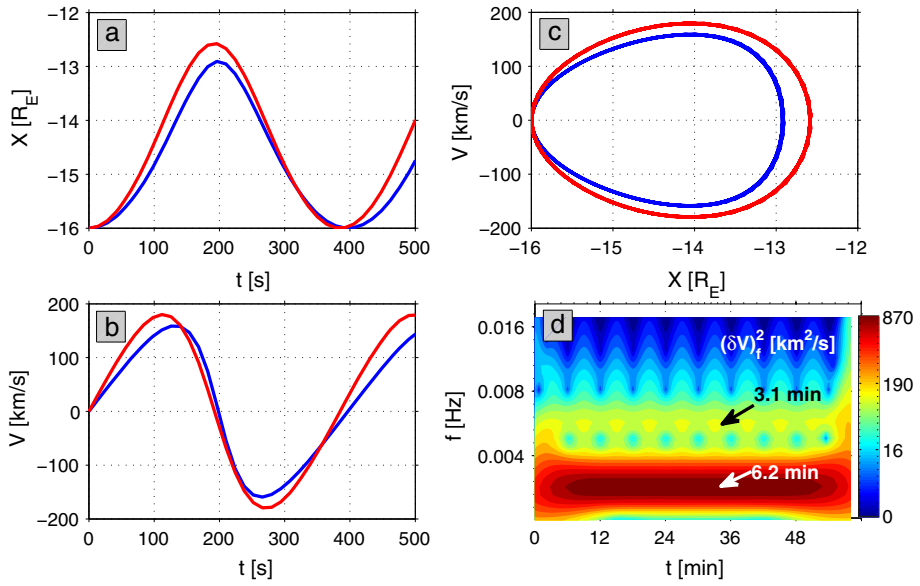

Figure 3. Anharmonic oscillation in an asymmetric potential of Figure 2e around the equilibrium position at $X = -14\ R_E$ at 6:21 UT: (a) coordinate x, (b) velocity v, (c) phase portrait (x,v), and (d) wavelet spectrum of v. Blue curves were calculated from force equation (A7), red curves from (A9).

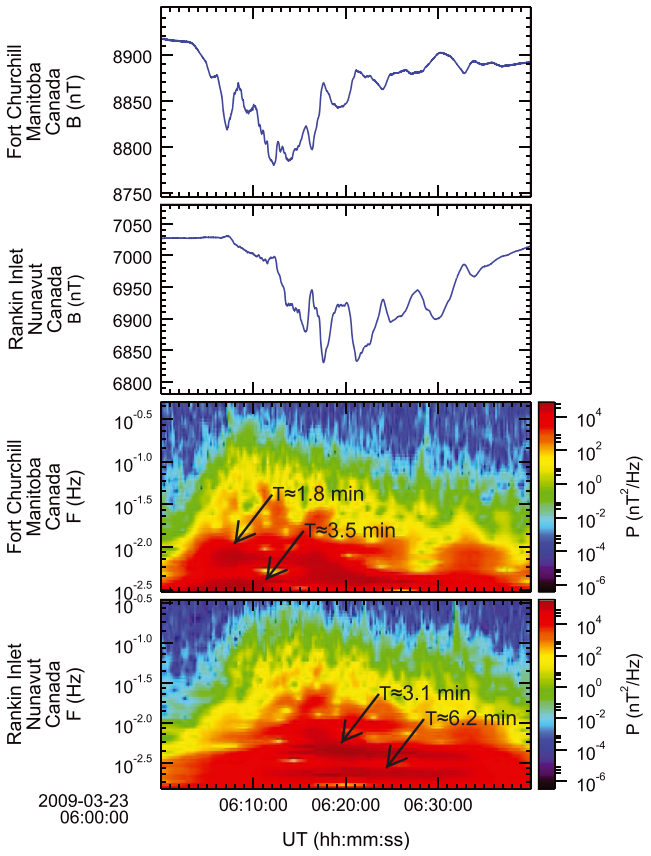

Figure 4. Ground B_H magnetic field component observed by magnetometers at (a and c) Fort Churchill, Manitoba, and (b and d) Rankin Inlet, Nunavut in Canada on 23 March 2009 between 6:00 and 6:40 UT, and their wavelet spectra.

Such coupling of different transmitting modes may further modify some parameters of the transmitted signal. Note that the amplitudes of the fundamental mode and of the first harmonic appear to be comparable in the ground observations, as is seen, e.g., in Figure 4d. The reason for the large amplitude of the first harmonic oscillation may be smaller ionospheric impedance on shorter magnetic field lines, when field line resonance effects [e.g., *Takahashi et al.*, 1996; *Glassmeier et al.*, 1999] are more dramatic. Thus, it is important to study how the magnetosphere-ionosphere transmission of the Pi2 pulsations down to Earth is organized in more detail.

Another important task would be to investigate whether the oscillatory flow braking could also effectively generate higher harmonics. The latter could explain the higher-frequency noise in the power spectrum of the ground magnetic field shown in Figure 4. Consider an axially symmetric magnetosphere, for simplicity, and consider the poloidal normal buoyancy modes that have zero north-south velocity at the equator and no nodes along the field lines (braking oscillations are of this type). Let $\omega_b(L)$ be the frequency of the thin filament oscillation centered at L. The normal mode that is proportional to $\exp(i(m\phi-\omega_b(L_0)t))$ peaks near L_0 and varies on a radial scale $(L_0/m)^{2/3}l^{1/3}$, where l is the scale length for variation of ω_b. In addition, that normal mode includes a buoyancy wave that may be able to propagate into the region of higher ω_b. If $\omega_b(L_1) = 2\omega_b(L_0)$ for L_1 within the range of the L_0-centered normal mode, then the first harmonic of that mode will resonate with the fundamental of the mode centered at L_1. Then the L_0-centered normal mode, which is the direct result of the BBF, will drive that fundamental mode, and the dominant oscillation seen near L_1 will be at ω_1=2ω_0, which may also be anharmonic if the amplitude is large enough.

Finally, we note that the progression of plasma sheet dipolarization farther downtail leads to tailward expansion of a flux pileup region and oscillatory braking accompanied by poleward drift of the associated auroral activity [*Panov et al.*, 2014a], when the flow oscillation period tends to increase on longer field lines farther out in the tail, which is in agreement with the MHD approximation predictions in *Wolf et al.* [2012]. Such plasma sheet development may lead to coexistence of eigenmodes with different oscillation periods. The question how such waves would interact with each other throughout the magnetosphere-ionosphere-plasmasphere system may be quite intriguing.

4. Conclusions

Applying thin filament theory to an AM03 model, magnetic field configuration adjusted to fit measurements made by five THEMIS probes for a period on 23 March 2009, we find that oscillatory flow braking may occur in an asymmetric potential. Oscillations in such a potential are anharmonic, exhibiting a power spectrum with peaks at both a fundamental frequency and a first harmonic. Thus, anharmonic oscillatory braking can explain the presence of the first harmonic in the Pi2 pulsations, which were simultaneously observed by magnetometers on the ground near the conjugate THEMIS footprints.

Appendix A: Estimation of Potential Well Motion Based On Magnetic Field Model

From equation (26) of *Wolf et al.* [2012], the earthward force on a thin filament containing one unit of magnetic flux is estimated as

$$F_x = -\frac{\pi\delta P}{B_{ze}}, \tag{A1}$$

where δ indicates the difference between the filament and the adjacent background. The condition of total pressure balance

$$P_b + \frac{B_b^2}{2\mu_o} = P_f + \frac{B_f^2}{2\mu_o} \tag{A2}$$

implies that the filament field strength in the center of the current sheet is given by

$$B_{ze} = \sqrt{B_{zeb}^2 - 2\mu_o\delta P}, \tag{A3}$$

where B_{zeb} is the corresponding background field. If the difference δB between the field strengths inside and outside the filament is small, then the difference in flux tube volume between the filament and adjacent background is

$$\delta V \approx -\int \frac{\delta B\, \mathrm{ds}}{B_b^2} \approx \frac{V_b}{2}\frac{\delta P}{P_b}\langle \beta_b \rangle, \tag{A4}$$

where

$$\langle \beta_b \rangle \equiv \frac{2\mu_o P_b}{V_b}\int \frac{\mathrm{ds}}{B_b^3}, \tag{A5}$$

and we used the first-order approximation to (A2) to write the second equality in (A4). Defining $K = PV^{\gamma}$, we can write, again to first order,

$$\frac{\delta K}{K} \approx \frac{\delta P}{P} + \gamma\frac{\delta V}{V} \approx \frac{\delta P}{P}\left(1 + \frac{\gamma\langle\beta\rangle}{2}\right). \tag{A6}$$

Substituting (A3) and (A6) in (A1) gives

$$F_{x1}(x_e, x_{eq}) = \frac{\pi Q(x_e)\, B_{zb}(x_e)\, \delta K(x_e, x_{eq})}{2\mu_o\sqrt{1 - Q(x_e)\, \delta K(x_e, x_{eq})}}, \tag{A7}$$

where

$$Q(x_e) = \frac{2\mu_o P_b(x_e)}{\left[1 + \frac{\gamma}{2}\langle\beta_b\rangle(x_e)\right] K_b(x_e)\, B_{zb}(x_e)^2}. \tag{A8}$$

The quantity $F_{x1}(x_e, x_{eq})$ is our estimate of the force on a filament whose equatorial crossing point has been displaced to x_e from its equilibrium position x_{eq}. In writing (A7), we have kept the nonlinear correction to B_{ze} but used the linear approximation in calculating the connection between δK and δP. Consequently, (A7) represents an overestimate of the nonlinear effect. Replacing the square root in (A7) with unity and writing

$$F_{x2}(x_e, x_{eq}) = \frac{\pi Q(x_e)\, B_{zb}(x_e)\, \delta K(x_e, x_{eq})}{2\mu_o} \tag{A9}$$

provides an underestimate. For both the force and the effective potential $U = -\int F_x\, \mathrm{d}x$, we therefore present calculations based on both (A7) and (A9) to obtain approximate bounds on the answer that would be obtained from a full nonlinear analysis.

Additional approximations involved in computing F_x, U, and velocity are the following:

1. The formula

$$\langle\beta\rangle \approx \frac{\beta_e}{1.8 + \sqrt{\beta_e}} \tag{A10}$$

   which is based on fitting field line integrals for both highly stretched and quasi-dipolar equilibrium magnetic field configurations.
2. Pressures are estimated from the magnetic field model.
3. The equatorial velocity of the filament is computed from

$$M\frac{\mathrm{d}V_x}{\mathrm{d}t} = F_x, \tag{A11}$$

   where M is the mass of the flux tube.

References

Angelopoulos, V. (2008), The THEMIS mission, *Space Sci. Rev.*, *141*, 5–34, doi:10.1007/s11214-008-9336-1.

Angelopoulos, V., C. F. Kennel, F. V. Coroniti, R. Pellat, M. G. Kivelson, R. J. Walker, C. T. Russell, W. Baumjohann, W. C. Feldman, and J. T. Gosling (1994), Statistical characteristics of bursty bulk flow events, *J. Geophys. Res.*, *99*, 21,257–21,280, doi:10.1029/94JA01263.

Auster, H. U., et al. (2008), The THEMIS fluxgate magnetometer, *Space Sci. Rev.*, *141*, 235–264, doi:10.1007/s11214-008-9365-9.

Baumjohann, W. (2002), Modes of convection in the magnetotail, *Phys. Plasmas*, *9*, 3665–3667, doi:10.1063/1.1499116.

Acknowledgments

We acknowledge NASA contract NAS5-02099 for the use of data from the THEMIS Mission and, specifically, for the use of FGM data supported through the German Ministry for Economy and Technology and the German Center for Aviation and Space (DLR) under contract 50 OC 0302. For the GBO/ASIs, we acknowledge S. Mende and E. Donovan, NASA contract NAS5-02099, and the CSA for logistical support in fielding and data retrieval from the GBO stations. The THEMIS data were obtained freely from Space Sciences Laboratory-University of California, Berkeley (ftp://themis.ssl.berkeley.edu/data/themis/). The authors gratefully acknowledge CANMOS, CARISMA, DTU, GIMA, MACCS, STEP, THEMIS, and USGS for the use of ground-based magnetic field data over Greenland and North America. The work was partly supported by the Austrian Science Fund (FWF) I429-N16 and by the Seventh Framework European Commission Programme (FP7, project 269198-Geoplasmas). Work at Rice was supported by the NASA Heliospheric Grand Challenge Research Program under grant NNX14AN55G and by the NSF GEM grant AGS-120367. The authors thank Shanshan Bao, Stanislav Sazykin, Aaron Schutza, Frank R. Toffoletto, and Jian Yang for insightful discussions.

The Editor thanks two anonymous reviewers for their assistance in evaluating this paper.

Baumjohann, W., G. Paschmann, and H. Luehr (1990), Characteristics of high-speed ion flows in the plasma sheet, *J. Geophys. Res.*, *95*, 3801–3809, doi:10.1029/JA095iA04p03801.
Baumjohann, W., G. Paschmann, T. Nagai, and H. Luehr (1991), Superposed epoch analysis of the substorm plasma sheet, *J. Geophys. Res.*, *96*, 11,605–11,608, doi:10.1029/91JA00775.
Baumjohann, W., M. Hesse, S. Kokubun, T. Mukai, T. Nagai, and A. A. Petrukovich (1999), Substorm dipolarization and recovery, *J. Geophys. Res.*, *104*, 24,995–25,000, doi:10.1029/1999JA900282.
Birn, J., M. Hesse, G. Haerendel, W. Baumjohann, and K. Shiokawa (1999), Flow braking and the substorm current wedge, *J. Geophys. Res.*, *104*, 19,895–19,904, doi:10.1029/1999JA900173.
Birn, J., R. Nakamura, E. V. Panov, and M. Hesse (2011), Bursty bulk flows and dipolarization in MHD simulations of magnetotail reconnection, *J. Geophys. Res.*, *116*, A01210, doi:10.1029/2010JA016083.
Chen, C. X., and R. A. Wolf (1999), Theory of thin-filament motion in Earth's magnetotail and its application to bursty bulk flows, *J. Geophys. Res.*, *104*, 14,613–14,626, doi:10.1029/1999JA900005.
Erickson, G. M., and R. A. Wolf (1980), Is steady convection possible in the Earth's magnetotail, *Geophys. Res. Lett.*, *7*, 897–900, doi:10.1029/GL007i011p00897.
Glassmeier, K.-H., C. Othmer, R. Cramm, M. Stellmacher, and M. Engebretson (1999), Magnetospheric field line resonances: A comparative planetology approach, *Surv. Geophys.*, *20*, 61–109, doi:10.1023/A:1006659717963.
Kaufmann, R. L., W. R. Paterson, and L. A. Frank (2005), Relationships between the ion flow speed, magnetic flux transport rate, and other plasma sheet parameters, *J. Geophys. Res.*, *110*, A09216, doi:10.1029/2005JA011068.
Kepko, L., M. G. Kivelson, and K. Yumoto (2001), Flow bursts, braking, and Pi2 pulsations, *J. Geophys. Res.*, *106*, 1903–1916, doi:10.1029/2000JA000158.
Kubyshkina, M., V. Sergeev, N. Tsyganenko, V. Angelopoulos, A. Runov, E. Donovan, H. Singer, U. Auster, and W. Baumjohann (2011), Time-dependent magnetospheric configuration and breakup mapping during a substorm, *J. Geophys. Res.*, *116*, A00I27, doi:10.1029/2010JA015882.
Lysak, R. L., Y. Song, M. D. Sciffer, and C. L. Waters (2015), Propagation of Pi2 pulsations in a dipole model of the magnetosphere, *J. Geophys. Res. Space Physics*, *120*, 355–367, doi:10.1002/2014JA020625.
Mann, I. R., et al. (2008), The upgraded CARISMA magnetometer array in the THEMIS era, *Space Sci. Rev.*, *141*, 413–451, doi:10.1007/s11214-008-9457-6.
McFadden, J. P., C. W. Carlson, D. Larson, M. Ludlam, R. Abiad, B. Elliott, P. Turin, M. Marckwordt, and V. Angelopoulos (2008), The THEMIS ESA plasma instrument and in-flight calibration, *Space Sci. Rev.*, *141*, 277–302, doi:10.1007/s11214-008-9440-2.
Mende, S. B., S. E. Harris, H. U. Frey, V. Angelopoulos, C. T. Russell, E. Donovan, B. Jackel, M. Greffen, and L. M. Peticolas (2008), The THEMIS array of ground-based observatories for the study of auroral substorms, *Space Sci. Rev.*, *141*, 357–387, doi:10.1007/s11214-008-9380-x.
Nakamura, R., D. N. Baker, D. H. Fairfield, D. G. Mitchell, R. L. McPherron, and E. W. Hones Jr. (1994), Plasma flow and magnetic field characteristics near the midtail neutral sheet, *J. Geophys. Res.*, *99*, 23,591–23,601, doi:10.1029/94JA02082.
Nakamura, R., et al. (2002), Motion of the dipolarization front during a flow burst event observed by Cluster, *Geophys. Res. Lett.*, *29*(20), 1942, doi:10.1029/2002GL015763.
Nishimura, Y., L. Lyons, S. Zou, V. Angelopoulos, and S. Mende (2010), Substorm triggering by new plasma intrusion: THEMIS all-sky imager observations, *J. Geophys. Res.*, *115*, A07222, doi:10.1029/2009JA015166.
Ohtani, S., Y. Miyashita, H. Singer, and T. Mukai (2009), Tailward flows with positive B_Z in the near-Earth plasma sheet, *J. Geophys. Res.*, *114*, A06218, doi:10.1029/2009JA014159.
Panov, E. V., M. V. Kubyshkina, R. Nakamura, W. Baumjohann, V. Angelopoulos, V. A. Sergeev, and A. A. Petrukovich (2013), Oscillatory flow braking in the magnetotail: THEMIS statistics, *Geophys. Res. Lett.*, *40*, 2505–2510, doi:10.1002/grl.50407.
Panov, E. V., W. Baumjohann, M. Kubyshkina, R. Nakamura, V. Sergeev, V. Angelopoulos, K. Glassmeier, and A. A. Petrukovich (2014a), On the increasing oscillation period of flows at the tailward retreating flux pileup region during dipolarization, *J. Geophys. Res. Space Physics*, *119*, 6603–6611, doi:10.1002/2014JA020322.
Panov, E. V., W. Baumjohann, R. Nakamura, M. Kubyshkina, K. Glassmeier, V. Angelopoulos, A. A. Petrukovich, and V. Sergeev (2014b), Period and damping factor of Pi2 pulsations during oscillatory flow braking in the magnetotail, *J. Geophys. Res. Space Physics*, *119*, 4512–4520, doi:10.1002/2013JA019633.
Pontius, D. H., Jr., and R. A. Wolf (1990), Transient flux tubes in the terrestrial magnetosphere, *Geophys. Res. Lett.*, *17*, 49–52, doi:10.1029/GL017i001p00049.
Schödel, R., R. Nakamura, W. Baumjohann, and T. Mukai (2001), Rapid flux transport and plasma sheet reconfiguration, *J. Geophys. Res.*, *106*, 8381–8390, doi:10.1029/2000JA900159.
Shiokawa, K., W. Baumjohann, and G. Haerendel (1997), Braking of high-speed flows in the near-Earth tail, *Geophys. Res. Lett.*, *24*, 1179–1182, doi:10.1029/97GL01062.
Shiokawa, K., et al. (1998), High-speed ion flow, substorm current wedge, and multiple Pi2 pulsations, *J. Geophys. Res.*, *103*, 4491–4508, doi:10.1029/97JA01680.
Takahashi, K., B. J. Anderson, and S.-I. Ohtani (1996), Multisatellite study of nightside transient toroidal waves, *J. Geophys. Res.*, *101*, 24,815–24,826, doi:10.1029/96JA02045.
Wolf, R. A., C. X. Chen, and F. R. Toffoletto (2012), Thin filament simulations for Earth's plasma sheet: Interchange oscillations, *J. Geophys. Res.*, *117*, A02215, doi:10.1029/2011JA016971.
Yang, J., R. A. Wolf, F. R. Toffoletto, S. Sazykin, and C.-P. Wang (2014), RCM-E simulation of bimodal transport in the plasma sheet, *Geophys. Res. Lett.*, *41*, 1817–1822, doi:10.1002/2014GL059400.

Erratum

In the originally published version of this article, the colors in figure 4 were not correctly rendered. The figure has since been corrected, and this version may be considered the authoritative version of record.